Inhibition of lipogenesis and induction of apoptosis by valproic acid in prostate cancer cells via the C/EBPα/SREBP-1 pathway

Bo Pang
Tianjin Medical University
Juanjuan Zhang
Tianjin Medical University
Jihong Yuan
Tianjin Medical University
Yanan Shi
Tianjin Medical University
Ling Qiao (qiaoling@tijmu.edu.cn)
Tianjin Medical University https://orcid.org/0000-0003-1160-9738

Research

Keywords: Valproic acid, Prostate cancer, Lipogenesis, Apoptosis, CCAAT/enhancer-binding protein α, Sterol regulatory element-binding protein-1

Posted Date: June 10th, 2020

DOI: https://doi.org/10.21203/rs.2.20628/v3

Abstract

Background: Lipid metabolism reprogramming is now accepted as a new hallmark of cancer. Hence, targeting the lipogenesis pathway may be a potential avenue for cancer treatment. Valproic acid (VPA) emerges as a promising drug for cancer therapy, however, the underlying mechanisms are not yet fully understood. This study aimed to investigate the effects and mechanisms of VPA on cell viability, lipogenesis, and apoptosis in human prostate cancer PC-3 cells.

Methods: The effects of VPA on the viability and migration of PC-3 cells were investigated using MTT cell viability assay and wound-healing assay. Oil-Red O staining was used to examine lipid droplets, and DAPI staining assay and Annexin V-FITC and PI double-staining assay were used to measure the extent of cell apoptosis. Quantitative real-time PCR and Western blotting were used to determine the expression of lipogenesis and apoptosis genes. Statistical and analytical data were analyzed with SPSS 17.0 Software, and statistical significance was set to * $P < 0.05$, ** $P < 0.01$, and *** $P < 0.001$ levels.

Results: The results showed that VPA significantly reduced lipid accumulation and induced apoptosis of PC-3 cells. Moreover, the expression of CCAAT/enhancer-binding protein α (C/EBPα), as well as sterol regulatory element binding protein 1 (SREBP-1) and its downstream effectors, including fatty acid synthase (FASN), acetyl CoA carboxylase 1 (ACC1), and antiapoptotic B cell lymphoma 2 (Bcl-2), markedly decreased in PC-3 cells after VPA administration. Mechanistically, the overexpression of C/EBPα rescued the levels of SREBP-1, FASN, ACC1, and Bcl-2, enhanced lipid accumulation and attenuated apoptosis of VPA-treated PC-3 cells. Conversely, knockdown of C/EBPα by siRNA further decreased lipid accumulation, enhanced apoptosis, and reduced the levels of SREBP-1, FASN, ACC1, and Bcl-2. In addition, SREBP-1a and 1c enhanced the expression of FASN and ACC1, but only SREBP-1a had a significant effect on Bcl-2 expression in VPA-treated PC-3 cells.

Conclusions: On the whole, it is concluded that VPA significantly inhibits cell viability via decreasing lipogenesis and inducing apoptosis via the C/EBPα/SREBP-1 pathway in PC-3 cells. Therefore VPA which targets lipid metabolism and apoptosis is a promising candidate for prostate cancer chemotherapy.

Background

Over the past decades, an increase in the incidence of various metabolic disorders, including type 2 diabetes mellitus, obesity, nonalcoholic fatty liver disease, atherosclerosis, thromboembolism, and cancer, has been closely associated with dysregulated lipid metabolism. Noticeably, the alteration of lipid metabolism has been increasingly recognized as a hallmark of cancer cells. Therefore, targeting lipid metabolic reprogramming is a potential cancer treatment strategy [1, 2]. Prostate cancer (PCa) is a common malignant tumor in the urinary system and the third leading cause of cancer-related death in men worldwide. PCa is well recognized as a lipid-enriched tumor, and an important biological feature of its progression is the dysregulation of lipid metabolism [3-5]. Previous studies indicate that inhibiting *de novo* lipogenesis via selectively deleting calcium/calmodulin-dependent protein kinase kinase 2,

activating AMP-activated protein kinase, or inhibiting fatty acid synthase (FASN), reduced cell growth in human PCa cells [6, 7].

Histone deacetylases are crucially involve in regulating the etiology and progression of prostate cancer. Valproic acid (VPA), a histone deacetylase inhibitor, has been used as an anticonvulsant and mood-stabilizing drug for more than 40 years. Previous study indicates that VPA suppresses adipogenesis and decreases the expression levels of peroxisome-proliferator-activated receptor γ, CCAAT/enhancer-binding protein α (C/EBPα), and FASN, all of which are key regulators of adipogenesis in adipocytes [8]. Treatment of ob/ob mice with VPA for 14 days results in decreased hepatic fat accumulation [9]. Recent studies have shown that VPA can suppress the malignancy of various cancers including prostate cancer, glioblastoma, and melanoma because it inhibits tumor growth and metastasis, induces differentiation and apoptosis, and enhances chemotherapy sensitivity [10-12]. Although a study indicates that VPA pretreatment suppresses PCa cell viability [13], its potential roles and, more importantly, the underlying mechanisms of its actions have not been extensively studied.

The present study aimed to gain insights into the antitumor mechanisms of VPA in PCa cells. The results showed that VPA inhibited cell viability in PC-3 cells through suppressing lipid accumulation and inducing cell apoptosis. It involved the key regulators of lipogenesis, including C/EBPα, sterol regulatory element binding protein-1 (SREBP-1) and their target genes. These findings might provide insights for PCa therapy targeting lipogenesis and apoptosis.

Methods

Cell culture and pharmacological intervention

The human prostate cancer PC-3 cells (obtained from Tianjin Medical University Cancer Institute and Hospital, National Clinical Research Center of Cancer, Tianjin, China) were cultured in RPMI 1640 medium (Gibco, CA, USA) with 10% (*v*/*v*) fetal bovine serum (Gibco, CA, USA) containing antibiotics (100 U/mL penicillin G and 100 mg/mL streptomycin) and incubated at 37˚C in 5% CO_2 humidified incubator. As per experimental requirements, PC-3 cells were treated with valproic acid (VPA, purchased from Sigma-Aldrich Chemicals, MO, USA) and then subjected to 3-(4,5-dimethylthiazol-2-yl)-2,5-diphenyltetrazolium bromide (MTT) cell viability assay, wound-healing assay, Oil-Red O staining, 4',6'-diamidino-2-phenyl-indole (DAPI) staining assay, Annexin V-FITC and propidium iodide (PI) double-staining assay, quantitative real-time polymerase chain reaction (qRT-PCR), and Western blotting analysis.

MTT cell viability assay

PC-3 cells were seeded in a 96-well plate at a density of 2×10^4 cells/well and incubated overnight, followed by treatment with the indicated concentrations of VPA. Then 10 μL of 5 mg/mL MTT (purchased from Amresco Inc., OH, USA) in phosphate-buffered saline (PBS) was added to each well and the cells were incubated in the dark for 4 h at 37˚C. The cell culture medium was replaced with 150 μL of dimethyl sulfoxide, and the mixture was stirred for 10 min. The optical density (OD) values for samples were

measured using a Pan-wavelength microplate reader at 570 nm. Each test included a blank containing a complete culture medium without cells. Triplicate wells were used for each sample, and the experiments were repeated at least three times to get means and standard deviations.

Wound-healing assay

The cell migration was examined using the wound-healing assay. PC-3 cells in each group were seeded into a 6-well plate. When the cells reached 60%-80% confluence, a wound was built across the cell monolayer using a BioClean 1000 μL plastic pipette tip. The cells were rinsed with PBS three times and incubated with fresh medium containing different dosages of VPA for another 4 days or 2.0 mM VPA for another 2, 4, and 6 days. The cell proliferation and migration into the wound area were photographed under an inverted microscope (Leica, Wetzlar, Germany) with 100× magnification. The relative migration rate was calculated using the following formula: relative migration rate = (distance between the gap at 0 h - distance between the gap at each time point)/distance between the gap at 0 h × 100%.

Oil-Red O staining

The adherent PC-3 cells grown on a glass coverslip at the bottom of a 6-well plate were fixed in 4% paraformaldehyde for 15 min and then analyzed with an Oil-Red O stain kit (Nanjing Jiancheng Bioengineering Institute, Nanjing, China) according to the supplier's instructions. After being rinsed in 60% isopropanol to remove unbound dye and counterstained with hematoxylin, the samples were taken photo of under an Olympus BX53 microscope (Olympus Corporation, Tokyo, Japan) equipped with a DP72 microscope digital camera and Image-Pro Plus 7.0 software. In order to quantify lipid accumulation, Oil-Red O was extracted with 100% isopropanol, and the light absorbance of the solution was measured at 520 nm.

Western blotting analysis

The cultured cells were collected and solubilized using protein lysis buffer. Lysates were cleared by centrifugation, and proteins were separated by gel electrophoresis. The membranes were blocked in PBS containing 0.1% Tween 20 and 5% (*w*/*v*) milk for 2 h at room temperature. The blots were first incubated with primary antibodies: anti-C/EBPα, anti-SREBP-1 (Abcam, Cambridge, UK), anti-Flag (Sigma-Aldrich Corp, St Louis, USA), anti-FASN, anti-acetyl CoA carboxylase 1 (ACC1), anti-B cell lymphoma 2 (Bcl-2), or anti-β-Actin (Proteintech, Wuhan, China), followed by incubation with the appropriate secondary antibody, that is, goat anti-rabbit IgG (H + L)-HRP or goat anti-mouse IgG (H + L)-HRP (RayBiotech, Beijing, China). The detection was performed using an enhanced chemiluminescence kit (Advansta, CA, USA).

DAPI staining assay

PC-3 cells (4×10^5 per well) were cultured in a 6-well plate, and nuclear morphology was tested using a DAPI staining assay. Following treatment with VPA (0, 1.0, 2.0, 5.0, and 10.0 mM) for 4 days, the cells were fixed with 4% paraformaldehyde for 15 min and permeabilized with 0.1% Triton X-100 for 2 min.

Then they were stained with 10 μg/mL DAPI (purchased from Roche Corporation, Basel, Switzerland) at 37°C in the dark for 10 min. The nuclear morphology was viewed under ultraviolet light, and the images were captured using an inverted fluorescence microscope (Leica, Wetzlar, Germany). Apoptotic cells were identified according to characteristic changes, including nuclear condensation, fragmentation, and presence of apoptotic bodies [14].

Annexin V-FITC and PI double-staining assay

PC-3 cells (4×10^5 per well) were seeded in a 6-well plate overnight and treated with various concentrations of VPA for 4 days. In order to measure the extent of cell apoptosis, an Annexin V-fluorescein isothiocyanate (FITC) and PI double-staining apoptosis detection kit was used according to the manufacturer's instructions (Sungene Biotech, Tianjin, China). In brief, the cells were harvested and suspended in 1× binding buffer. Then, 100 μL of the cell suspension was incubated with 5 μL of Annexin V-FITC for 10 min, followed by incubation with 5 μL of PI solution for another 5 min. The labeled cells were then assessed by flow cytometry and analyzed using Cellquest 6.0 (BD Biosciences, NJ, USA) [15].

Cell transfection

In brief, the PC-3 cells seeded in a 6-well, 12-well, or 96-well plate were transfected using Lipofectamine 3000 transfection reagent (Invitrogen, CA, USA) according to the manufacturer's protocol. The following plasmids were used: pcDNA3-C/EBPα (a gift from Dr. Hong Yin), pcDNA3.1-2xFlag-SREBP-1a, and pcDNA3.1-2xFlag-SREBP-1c (from Addgene, MA, USA). The siRNA against C/EBPα (in short, Si-C/EBPα) and the negative control siRNA (in short, Si-Control) were designed and synthesized by RiboBio Company (Guangzhou, China). The siRNA against C/EBPα used in the present study was as follows: sense: 5'-GGAGCUGACCAGUGACAAUdTdT-3'; antisense: 5'-AUUGUCACUGGUCAGCUCCdTdT-3'.

Quantitative real-time PCR

Total RNA was extracted from PC-3 cells after transfection with C/EBPα-expressing plasmid or Si-C/EBPα and/or treatment with VPA (2.0 mM) using an E.Z.N.A. HP Total RNA Extraction Kit (Omega Bio-Tek, GA, USA). Reverse transcription reactions were performed with 2.0 μg total RNA using a RevertAid First Strand cDNA Synthesis Kit and oligo (dT) primers (Fermentas Inc., Burlington, Ontario, Canada) according to the manufacturer's protocol. The abundance of mRNA was detected using an SYBR Green real-time PCR kit according to the manufacturer's instructions (Sangon Biotech, Shanghai, China). *β-Actin* reference gene was amplified in separate triplicate reactions for each sample and the average Ct value was calculated for the quantification analysis. The relative transcript quantities of *SREBP-1a* and *SREBP-1c* were measured using the comparative Ct ($2^{-\Delta\Delta Ct}$) method. The measurement was performed in three independent experiments and each with three replicates. The sequences of the primer pairs were as follows: *SREBP-1a*: 5¢-CGGCGCTGCTGACCGACATC-3¢ and 5¢-CCCTGCCCCACTCCCAGCAT-3¢; *SREBP-1c*: 5¢-GCGCAGATCGCGGAGCCAT-3¢ and 5¢-CCCTGCCCCACTCCCAGCAT-3¢; and *β-Actin*: 5¢-CCAGAGATGGCCACGGCTGCT-3¢ and 5¢-TCCTTCTGCATCCTGTCGGCA-3¢.

Statistical analysis

The experiments were repeated at least three times, and data were analyzed using SPSS (version 17.0; SPSS, Inc., IL, USA). All data were expressed as the mean ± *S.D.* A statistical analysis between two groups was performed using the Student¢s *t*-test. One-way analysis of variance was used for the bar plots containing three or more groups. $^{*}P < 0.05$, $^{**}P < 0.01$, and $^{***}P < 0.001$ indicate significant differences, whereas the nonsignificant difference is denoted by NS.

Results

Effects of VPA on PC-3 cell viability

The incidence of PCa exhibits an increasing trend in recent years. Previous studies indicated that VPA is a potential suppressor of the growth of PCa cells [10, 13, 16]. To test whether the growth inhibition was dose dependent, PC-3 cells were treated with different concentrations of VPA (ranging from 0.5 to 10.0 mM) for 4 days, followed by the MTT cell viability assay. The result showed that the growth of PC-3 cells was slow after VPA administration. The growth ability decreased in a dose-dependent manner, ranging from 7.52% for the low VPA concentration (0.5 mM) up to 76.7% for the high VPA concentration (10.0 mM) compared to the control cells (Fig. 1a, left). Meanwhile, PC-3 cells were treated with 2.0 mM VPA over a time course of 1, 2, 4, and 6 days. As shown in Figure 1a (right), VPA inhibited the growth of PC-3 cells significantly in a time-dependent manner, ranging from 9.73% for 1 day up to 64.4% for 6 days compared to the control cells. The inhibitory effect of VPA on PC-3 cell migration was confirmed by the wound-healing assay. Consistently, similar results were observed, and showed that VPA markedly delayed the wound closure of PC-3 cells (Fig. 1b and 1c). Altogether, the results demonstrate that VPA remarkably prevents the PC-3 cell viability.

Effects of VPA on lipogenesis in PC-3 cells

Cancer is a disorder characterized by increased metabolic activity leading to enhanced cell growth and proliferation. Alterations in lipid metabolism are one of the main features in cancer cells [5, 17, 18]. Therefore, the functional effects of VPA on lipogenesis in PC-3 cells were determined in this study. PC-3 cells were treated with 0, 0.5, 1.0, 2.0, and 5.0 mM VPA for 4 days, followed by Oil-red O staining and Western blotting analysis. The results showed that VPA decreased lipid deposition in PC-3 cells in a dose-dependent manner, as evidenced by Oil-red O staining (Fig. 2a, b). The expression levels of FASN and ACC1, which are the key enzymes of *de novo* lipogenesis, were significantly suppressed in a dose-dependent manner when PC-3 cells were cultured in a medium containing VPA (Fig. 2c, d).

Effects of VPA on apoptosis in PC-3 cells

VPA is now a promising anticancer compound due to its pharmacological effects on lipogenesis and apoptosis [8-10]. Therefore, the degree of apoptosis for VPA-treated PC-3 cells was analyzed by DAPI staining assay and Annexin V-FITC and PI double-staining assay. DAPI staining showed that the nuclear

morphology of VPA-treated cells, including the rippled surface of nuclei, chromatin condensation, and nuclear fragmentation, presented more and brighter blue fluorescence compared to the control cells, suggesting the typical characteristics of apoptosis (Fig. 3a). To further investigate the apoptosis of PC-3 cells induced by VPA, the apoptotic cells were quantified with a flow cytometer using Annexin V-FITC and PI double-staining. As shown in Figure 3b and 3c, the percentage of apoptotic cells induced by VPA exhibited a significant increase compared to the control cells (from 8.89% to 22.73%). Consistent with these results, Western blotting analysis showed that the expression level of Bcl-2 in VPA-treated PC-3 cells significantly decreased in a dose-dependent manner (Fig. 3d, e). Collectively, the results above suggest that VPA suppresses the growth of PC-3 cells by inhibiting lipogenesis and inducing apoptosis.

C/EBPα regulated lipogenesis and apoptosis-related genes in VPA-treated PC-3 cells

C/EBPα and SREBP-1 play pivotal roles in lipid metabolism by inducing the transcription of genes related to lipogenesis [8, 19]. Recent studies revealed that C/EBPα and SREBP-1 are markedly upregulated in human cancers, providing the mechanistic link between lipid metabolism alterations and malignancies [18, 20, 21]. To identify the metabolic changes occurring during VPA-induced antitumor progression, the expression levels of C/EBPα and SREBP-1 were determined by Western blotting analysis. As shown in Figure 4a and 4b, the expression levels of C/EBPα and SREBP-1 were significantly suppressed in PC-3 cells treated with VPA in a dose-dependent manner. Furthermore, the ectopic expression of C/EBPα inverted the downregulation of SREBP-1, FASN, ACC1, and Bcl-2 caused by VPA, as shown by Western blotting analysis (Fig. 4c, d). The siRNA strategy was used to specifically knockdown C/EBPα and Western blotting analysis result confirmed the dramatic C/EBPα downregulation in PC-3 cells. As expected, the decrease of protein levels of SREBP-1, FASN, ACC1, and Bcl-2 was amplified in PC-3 cells transfected with siRNA sequences specifically against C/EBPα (in short, Si-C/EBPα) compared to the cells transfected with scrambled control siRNA (in short, Si-Control) (Fig. 4e, f). These results indicate that C/EBPα plays an important role in expression of SREBP-1, FASN, ACC1, and Bcl-2 in VPA-treated PC-3 cells. Hence it is presumed that the C/EBPα/SREBP-1 pathway might be involved in the suppression of lipogenesis and induction of apoptosis in PC-3 cells after VPA administration.

Effects of SREBP-1a and SREBP-1c on expression of lipogenesis and apoptosis-related genes in VPA-treated PC-3 cells

The changes in cell metabolism and growth are closely linked through SREBPs. The SREBP family consists of three subtypes: SREBP-1a, SREBP-1c, and SREBP-2. SREBP-1a and SREBP-1c are derived from a single gene using of alternative transcription start sites. In general, SREBP-1c seems to act more specifically on the genes involved in fatty acid synthesis, while SREBP-1a affects a large number of genes involved in the regulation of lipid metabolism, cell proliferation, differentiation, and death [19-22]. Importantly, our previous study indicates that C/EBPα enhances SREBP-1a activation at the transcriptional level [23]. Hence the present study examined the effects of C/EBPα on the transcriptional levels of SREBP-1a and SREBP-1c in PC-3 cells in the presence of VPA. PC-3 cells were transfected with C/EBPα-expressing plasmid or Si-C/EBPα for 48 h in the presence of VPA (2.0 mM), and the

transcriptional levels of SREBP-1a and SREBP-1c were tested by qRT-PCR analysis. The results demonstrated that ectopic expression of C/EBPα neutralized the suppression of SREBP-1a and SREBP-1c activation, while Si-C/EBPα exerted an inhibitory effect and enhanced suppression in PC-3 cells exposed to VPA (Fig. 5a). In addition, the ectopic expression of SREBP-1a rescued the expression of FASN and ACC1 as well as the expression of Bcl-2 in VPA-treated cells (Fig. 5b, c). Different from SREBP-1a, the ectopic expression of SREBP-1c rescued the expression of FASN and ACC1 but had no effect on Bcl-2 expression in VPA-treated cells (Fig. 5d, e).

Effects of the C/EBPα/SREBP-1 pathway on lipogenesis and apoptosis in VPA-treated PC-3 cells

Subsequently, the effects of C/EBPα and SREBP-1 on PC-3 cell viability, lipogenesis, and apoptosis were examined. MTT cell viability assay exhibited an apparent increase in C/EBPα- or SREBP-1-expressing cells and a sharp decrease in Si-C/EBPα cells compared to the control cells (Fig. 6a). The ectopic expression of C/EBPα or SREBP-1 led to a significant increase in lipid accumulation in PC-3 cells treated with VPA compared to the control cells. The loss of lipids and smaller lipid droplets as a result of C/EBPα knockdown was also confirmed by Oil-red O staining (Fig. 6b, c). The ectopic expression of C/EBPα or SREBP-1 partially suppressed VPA-induced apoptosis in PC-3 cells, whereas Si-C/EBPα enhanced it (Fig. 6d, e). Taken together, it is concluded that VPA treatment significantly decreases lipid accumulation and induces apoptosis as a result of the inhibition of C/EBPα as well as SREBP-1 and its target gene expression. VPA-triggered suppression of the C/EBPα/SREBP-1 pathway might provide mechanistic insights and offer a novel therapeutic strategy for PCa.

Discussion

Metabolic reprogramming not only promotes cancer cell plasticity but also provides novel insights for treatment strategies. Altered lipid metabolism is increasingly recognized as a signature of cancer cells, and the proteins involved in this process can be promising chemotherapeutic targets for cancer treatment [24-27]. A link between PCa progression and lipogenesis has been investigated in the past few decades. Several recent studies suggest that the activation of *de novo* lipogenesis and cholesterogenesis induces PCa cell proliferation and promotes PCa development and progression. Hence, targeting the lipogenesis pathway may be a promising avenue for PCa treatment [26-29].

VPA is known as a histone deacetylase inhibitor and an anticonvulsant and mood-stabilizing drug. It has been reported as a potent and promising anticancer drug candidate [10-12]. In the present study, the anticancer effects of VPA on human prostate cancer PC-3 cells were detected using MTT cell viability assay and wound-healing assay. The results indicated that VPA inhibited cell growth significantly in a dose-dependent and time-dependent manner. Moreover, VPA significantly inhibited lipogenesis and induced cellular apoptosis in PC-3 cells. Further assays were performed to analyze the underlying molecular mechanisms. C/EBPα and SREBP-1 are crucial factors controlling lipogenesis. It is reported that VPA suppresses the accumulation of intracellular triacylglycerol and decreases the expression level of C/EBPα [8]. In addition, a growing amount of evidence suggests that aberrant SREBP-1 activity can

contribute to cancer [30]. A previous study indicates that SREBP-1 was overexpressed and involved in the transcriptional regulation of fatty acid synthesis through the altered expression of FASN in prostate cancer cells [19]. Hence, the present study focused on C/EBPα and SREBP-1. The results showed that the expression levels of C/EBPα and SREBP-1, as well as their target genes FASN, ACC1, and Bcl-2, decreased significantly after VPA treatment.

An adapted “metabolic switch” accompanies most physiological and pathological changes in cellular functions. Lipid metabolism is essential for cancer cells and is associated with the regulation of a variety of key cellular processes and functions [31-33]. The cellular metabolites can directly or indirectly regulate the apoptotic machinery. Metabolism is emerging as one of the key factors contributing to the dysregulation of apoptosis in cancer [34]. The suppression of C/EBPα inhibits cell proliferation by inducing G1-phase arrest and apoptosis [20]. Emerging evidences indicate that SREBP-1a couples lipid synthesis to cell progression and apoptosis [28, 35]. A recent study shows that SREBP-1a regulates antiapoptotic factor apoptosis inhibitor 6 (Api6) besides regulating lipid metabolism in response to different nutrient levels. Consistently, the results revealed that the antiapoptotic Bcl-2 expression regulated by SREBP-1a might play a role in the apoptosis of VPA-treated PC-3 cells. The study suggests distinct effects of the two SREBP-1 isoforms, with SREBP-1a playing a more important role in VPA-induced apoptosis in PC-3 cells.

PCa is the most prevalent urological cancer and the heterogeneous nature of PCa is well known [36, 37]. The castration-resistant prostate cancer (CRPC) is associated with a poor prognosis and the treatment of CRPC is still clinically difficult. The molecular targets for CRPC remain unclear and therapeutic approaches for patients with CRPC remain less well understood. A better understanding of the molecular biology of CRPC will lead to a dramatic increase in the treatment of patients. In the present study, the castration-resistant prostate cancer PC-3 cell line was used and the results demonstrate that VPA is a potential avenue for CRPC treatment.

Conclusions

Together, the present study indicates that VPA inhibits prostate cancer growth via the C/EBPα/SREBP-1 pathway targeting lipogenesis and apoptosis. Therefore, blocking histone deacetylases (HDAC) or fatty acid biosynthesis could be a potential treatment for PCa. Because of the cellular heterogeneity observed among prostate cancer patients, it would be more convincing if we use more prostate cancer cell lines (C4-2, 22Rv1 or DU145 etc.) to explore the effects and mechanism of VPA. Our results are expected to provide new insights into the treatment of prostate cancer, find potential drug target proteins involved in dysregulated lipid metabolism and apoptosis, and explore the possibility of combined treatment targeting lipid metabolism and apoptosis in prostate cancer.

Declarations

Acknowledgements

We would like to thank MedSci for reviewing and providing professional editing services for the manuscript.

Authors' contributions

BP performed experiments, analyzed data and helped write the manuscript. JZ, JY and YS helped design and perform experiments. LQ conceived the project, designed the overall research, wrote the manuscript, mentored and supervised participants. All authors have read, commented on, and approved the final manuscript.

Funding

This study was supported by the National Natural Science Foundation of China (81370955, 81300664, and 81800767) and the Tianjin Natural Science Foundation (18JCYBJC25500).

Availability of data and materials

The authors confirm that all materials described in the manuscript are fully available to any scientist wishing to use them, without restriction.

Ethics approval

Not applicable.

Consent for publication

All authors agree to publish this article in the journal of Lipids in Health and Disease.

Competing interests

The authors declare that they have no competing interests

Author details

NHC Key Laboratory of Hormones and Development (Tianjin Medical University), Tianjin Key Laboratory of Metabolic Diseases, Tianjin Medical University Chu Hsien-I Memorial Hospital & Tianjin Institute of Endocrinology, Tianjin Medical University, Tianjin 300134, China.

Abbreviations

ACC1: acetyl-coenzyme A carboxylase 1; Bcl-2: antiapoptotic B cell lymphoma 2; Api6: antiapoptotic factor apoptosis inhibitor 6; C/EBPα: CCAAT/enhancer-binding protein α；DAPI: 4', 6'-diamidino-2-phenyl-indole; FASN: fatty acid synthase; FITC: fluorescein isothiocyanate; MTT: 3-(4, 5-dimethylthiazol-2-yl)-2, 5-diphenyltetrazolium bromide; OD: optical density; PBS: phosphate-buffered saline; PI: propidium iodide; PCa: prostate cancer; qRT-PCR: quantitative real-time PCR; SREBP-1: sterol regulatory element binding

protein 1; SREBP-1a: sterol regulatory element binding protein-1a; SREBP-1c: sterol regulatory element binding protein-1c; VPA: valproic acid

References

1. Nickels JT Jr. New links between lipid accumulation and cancer progression. J Biol Chem. 2018; 293 (17): 6635-6636.
2. Guri Y, Colombi M, Dazert E, et al. mTORC2 Promotes Tumorigenesis via Lipid Synthesis. Cancer Cell. 2017; 32(6): 807-823.
3. Gordon JA, Noble JW, Midha A, et al. Upregulation of Scavenger Receptor B1 Is Required for Steroidogenic and Nonsteroidogenic Cholesterol Metabolism in Prostate Cancer. Cancer Res. 2019; 79(13): 3320-3331.
4. Yue S, Li J, Lee SY, et al. Cholesteryl ester accumulation induced by PTEN loss and PI3K/AKT activation underlies human prostate cancer aggressiveness. Cell Metab. 2014; 9(3): 393-406.
5. Singh KB, Kim SH, Hahm ER, et al. Prostate cancer chemoprevention by sulforaphane in a preclinical mouse model is associated with inhibition of fatty acid metabolism. Carcinogenesis. 2018; 39(6): 826-837.
6. Zadra G, Ribeiro CF, Chetta P, et al. Inhibition of de novo lipogenesis targets androgen receptor signaling in castration-resistant prostate cancer. Proc Natl Acad Sci U S A. 2019; 116(2): 631-640.
7. Penfold L, Woods A, Muckett P, et al. CAMKK2 Promotes Prostate Cancer Independently of AMPK via Increased Lipogenesis. Cancer Res. 2018; 78(24): 6747-6761.
8. Yuyama M, Fujimori K. Suppression of adipogenesis by valproic acid through repression of USF1-activated fatty acid synthesis in adipocytes. Biochem J. 2014; 459(3): 489-503.
9. Avery LB, Bumpus NN. Valproic acid is a novel activator of AMP-activated protein kinase and decreases liver mass, hepatic fat accumulation, and serum glucose in obese mice. Mol Pharmacol. 2014; 85(1): 1-10.
10. Kawashima N, Nishimiya Y, Takahata S, et al. Induction of Glycosphingolipid GM3 Expression by Valproic Acid Suppresses Cancer Cell Growth. J Biol Chem. 2016; 291(41): 21424-21433.
11. Zapotocky M, Mejstrikova E, Smetana K, et al. Valproic acid triggers differentiation and apoptosis in AML1/ETO-positive leukemic cells specifically. Cancer Lett. 2012; 319(2): 144-153.
12. Roos WP, Jöst E, Belohlavek C, et al. Intrinsic anticancer drug resistance of malignant melanoma cells is abrogated by IFN-β and valproic acid. Cancer Res. 2011; 71(12): 4150-60.
13. Makarević J, Rutz J, Juengel E, et al. HDAC Inhibition Counteracts Metastatic Re-Activation of Prostate Cancer Cells Induced by Chronic mTOR Suppression. Cells. 2018; 7(9): pii: E129.
14. Liu L, Gao H, Wang H, et al. Catalpol promotes cellular apoptosis in human HCT116 colorectal cancer cells via microRNA-200 and the downregulation of PI3K-Akt signaling pathway. Oncol Lett. 2017; 14(3): 3741-3747.

15. Wang, H. Li, X. Wang, et al. Alisol B-23-acetate, a tetracyclic triterpenoid isolated from Alisma orientale, induces apoptosis in human lung cancer cells via the mitochondrial pathway. Biochem Biophys Res Commun. 2018; 505(4): 1015-1021.
16. Chou YW, Chaturvedi NK, Ouyang S, et al. Histone deacetylase inhibitor valproic acid suppresses the growth and increases the androgen responsiveness of prostate cancer cells. Cancer Lett. 2011; 311(2): 177-86.
17. Xie H, Simon MC. Oxygen availability and metabolic reprogramming in cancer. J Biol Chem. (2017); 292(41): 16825-16832.
18. Guo D, Reinitz F, Youssef M, et al. An LXR agonist promotes glioblastoma cell death through inhibition of an EGFR/AKT/SREBP-1/LDLR-dependent pathway. Cancer Discov. 2011; 1(5): 442-56.
19. Walker AK, Jacobs RL, Watts JL, et al. A conserved SREBP-1/phosphatidylcholine feedback circuit regulates lipogenesis in metazoans. Cell. 2011; 147(4): 840-52.
20. Lee J, Imm JY, Lee SH. β-Catenin Mediates Anti-adipogenic and Anticancer Effects of Arctigenin in Preadipocytes and Breast Cancer Cells. J Agric Food Chem. 2017; 65(12): 2513-2520.
21. .Li W, Tai Y, Zhou J, et al. Repression of endometrial tumor growth by targeting SREBP1 and lipogenesis. Cell Cycle. 2012; 11(12): 2348-58.
22. Shao W, Espenshade PJ. Expanding roles for SREBP in metabolism. Cell Metab. 2012; 16(4): 414-419.
23. Qiao L, Wu Q, Lu X, et al. SREBP-1a activation by HBx and the effect on hepatitis B virus enhancer II/core promoter. Biochem Biophys Res Commun. 2013; 432(4): 643-649.
24. Li, M. Li, J. Hu, et al., The microRNA-182-PDK4 axis regulates lung tumorigenesis by modulating pyruvate dehydrogenase and lipogenesis. Oncogene. 2017; 36(7): 989-998.
25. Gomes AS, Ramos H, Soares J, et al. p53 and glucose metabolism: an orchestra to be directed in cancer therapy. Pharmacol Res. 2018; 131: 75-86.
26. Zadra G, Photopoulos C, Tyekucheva S, et al. A novel direct activator of AMPK inhibits prostate cancer growth by blocking lipogenesis. EMBO Mol Med. 2014; 6(4): 519-38.
27. Dasgupta S, Putluri N, Long W, et al. Coactivator SRC-2-dependent metabolic reprogramming mediates prostate cancer survival and metastasis. J Clin Invest. 2015; 125(3): 1174-88.
28. O'Malley J, Kumar R, Kuzmin AN, et al. Lipid quantification by Raman microspectroscopy as a potential biomarker in prostate cancer. Cancer Lett. 2017; 397: 52-60.
29. Chen J, Guccini I, Mitri DD, et al. Compartmentalized activities of the pyruvate dehydrogenase complex sustain lipogenesis in prostate cancer. Nat Genet. 2018; 50(2): 219-228.
30. Talebi A, Dehairs J, Rambow F, et al. Sustained SREBP-1-dependent lipogenesis as a key mediator of resistance to BRAF-targeted therapy. Nat Commun. 2018; 9(1): 2500.
31. Iwamoto H, Abe M, Yang Y, et al. Cancer Lipid Metabolism Confers Antiangiogenic Drug Resistance. Cell Metab. 2018; 28(1): 104-117.

32. Stockwell BR, Friedmann Angeli JP, Bayir H, et al. Ferroptosis: A Regulated Cell Death Nexus Linking Metabolism, Redox Biology, and Disease. Cell. 2017; 171(2): 273-285.
33. Pommier AJ, Alves G, Viennois E, et al. Liver X Receptor activation downregulates AKT survival signaling in lipid rafts and induces apoptosis of prostate cancer cells. Oncogene. 2010; 29(18): 2712-23.
34. Matsuura K Canfield K, Feng W, et al., Metabolic Regulation of Apoptosis in Cancer. Int Rev Cell Mol Biol. 2016; 327: 43-87.
35. Im SS, Osborne TF. Protection from bacterial-toxin-induced apoptosis in macrophages requires the lipogenic transcription factor sterol regulatory element binding protein 1a. Mol Cell Biol. 2012; 32(12): 2196-202.
36. Abida W, Cyrta J, Heller G, et al. Genomic correlates of clinical outcome in advanced prostate cancer. Proc Natl Acad Sci U S A. 2019, 116(23): 11428-11436.
37. Li Q, Deng Q, Chao HP, et al. Linking prostate cancer cell AR heterogeneity to distinct castration and enzalutamide responses. Nat Commun. 2018, 9(1): 3600.

Figures

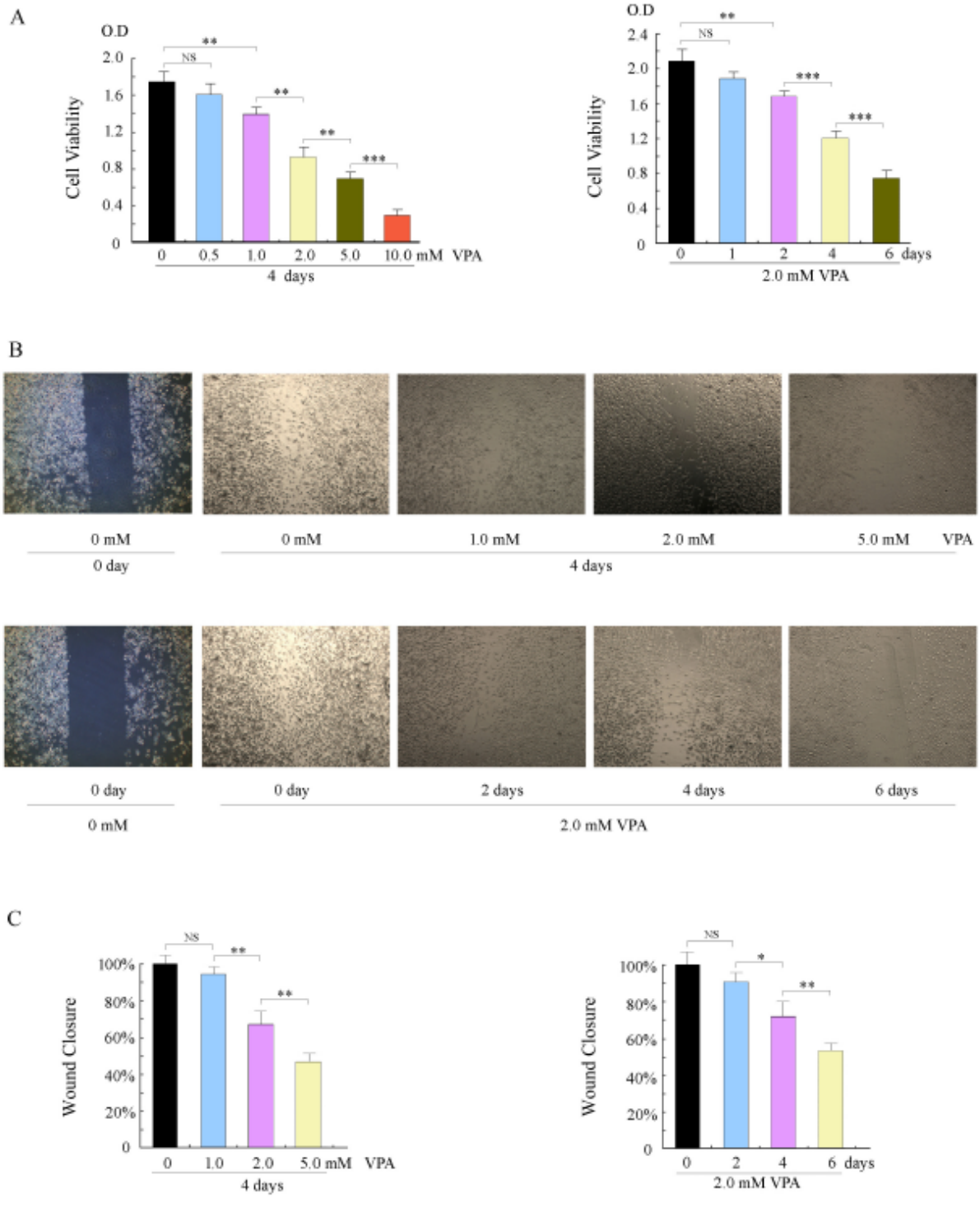

Figure 1

Effects of VPA on PC-3 cell viability. (a) The viability of PC-3 cells after treatment with increasing concentrations of VPA (0, 0.5, 1.0, 2.0, 5.0, and 10.0 mM) for 4 days was measured using the MTT cell viability assay. VPA significantly inhibited cell growth in a dose-dependent manner (left). The viability of PC-3 cells treated with 2.0 mM VPA for 1, 2, 4 and 6 days was measured at the end of 6 days. VPA significantly inhibited cell growth in a time-dependent manner (right). (b) Representative PC-3 cell wound

healing width images. The migration of PC-3 cells treated with various concentrations of VPA for 4 days (up) or 2.0 mM VPA for 0, 2, 4, and 6 days (down) was assessed using wound-healing assay. The images were taken at the end of 4 days (up) or 6 days (down). (c) The viability was calculated according to the width of wound closure. Data are expressed as mean ± S.D, n = 3. Statistically significant differences are indicated as follows: NS (no significance), *P < 0.05, **P < 0.01, and ***P < 0.001.

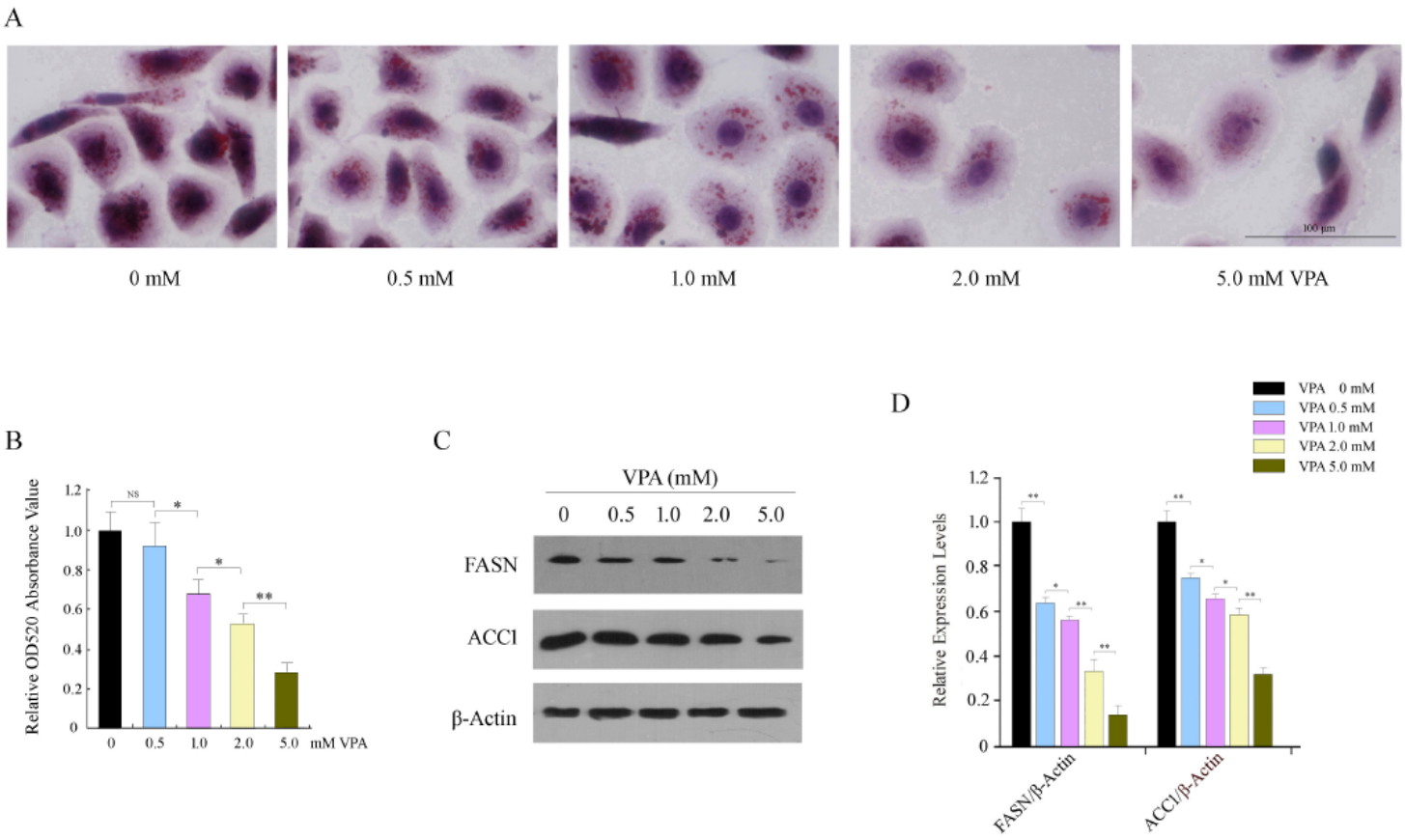

Figure 2

Efects of VPA on lipogenesis in PC-3 cells. (a) Effect of VPA on lipid storage in PC-3 cells was detected by Oil-Red O staining. (b) Oil-Red O extracted with isopropanol was measured at OD520. Scale bar = 100 μm. (c) Western blotting detection of the lipogenic gene expression of PC-3 cells after treatment with various concentrations of VPA. β-Actin was used as a loading control. (d) A semi-quantitative analysis of lipogenic gene expression was performed using ImageJ.

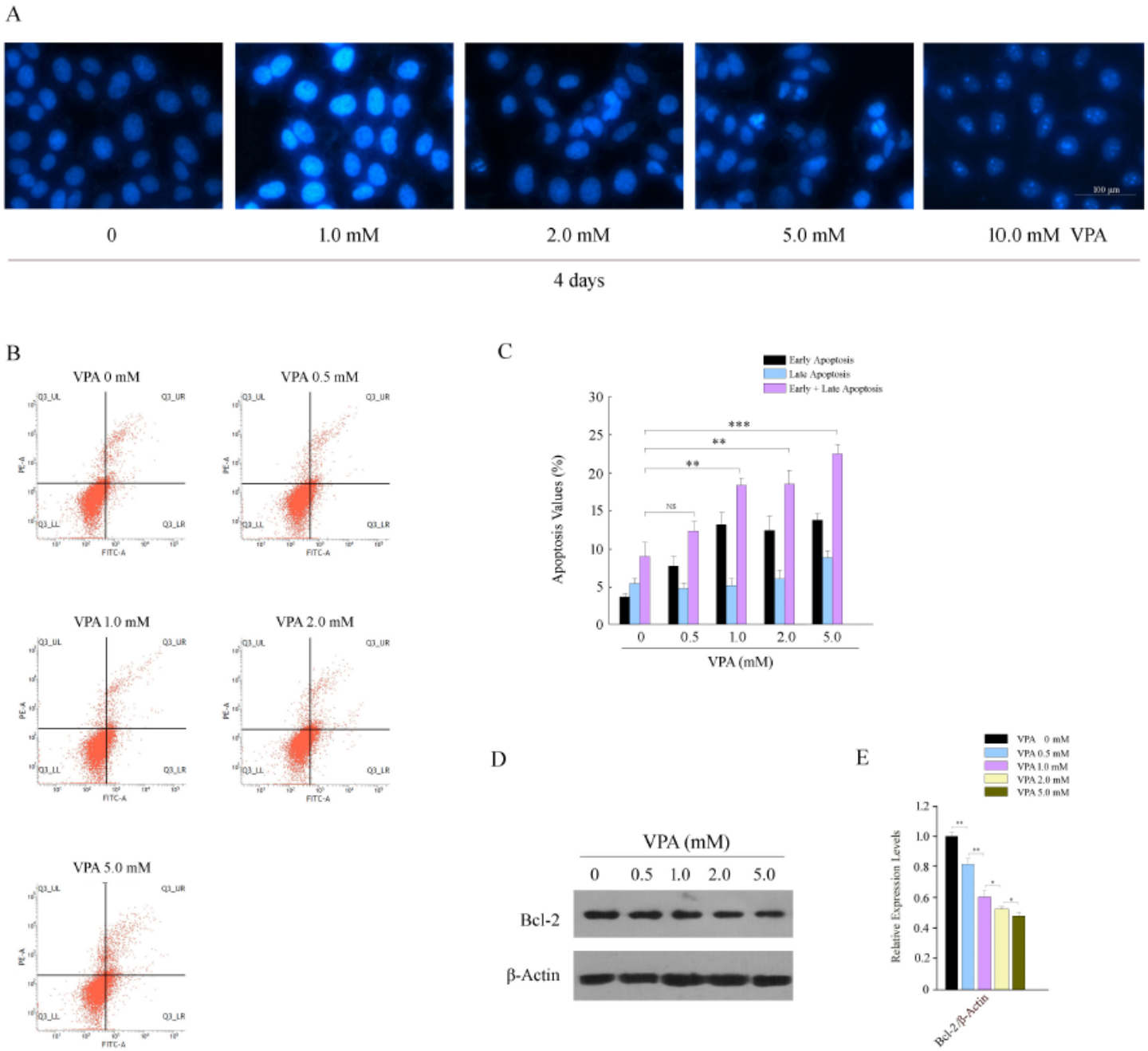

Figure 3

Effects of VPA on apoptosis in PC-3 cells. (a) PC-3 cells were incubated with various concentrations of VPA for 4 days, and the changes in nuclear morphology were evaluated using DAPI staining. (b) PC-3 cells were treated with 0 (control), 0.5, 1.0, 2.0, and 5.0 mM VPA. The apoptotic rate was measured by flow cytometry with Annexin V-FITC and PI double-staining. PI, Propidium iodide. (c) Summary of the percentage of apoptotic cells when treated with various concentrations of VPA. (d) Level of Bcl-2 in PC-3 cells was analyzed by Western blotting analysis. β-Actin was used as a loading control. (e) The fold-change was calculated based on the densitometric analysis of the band intensities. All experiments were

performed three times. Data are expressed as mean ± S.D. Statistically significant differences are indicated as fellows: NS (no significance), *P < 0.05, **P < 0.01, and ***P < 0.001.

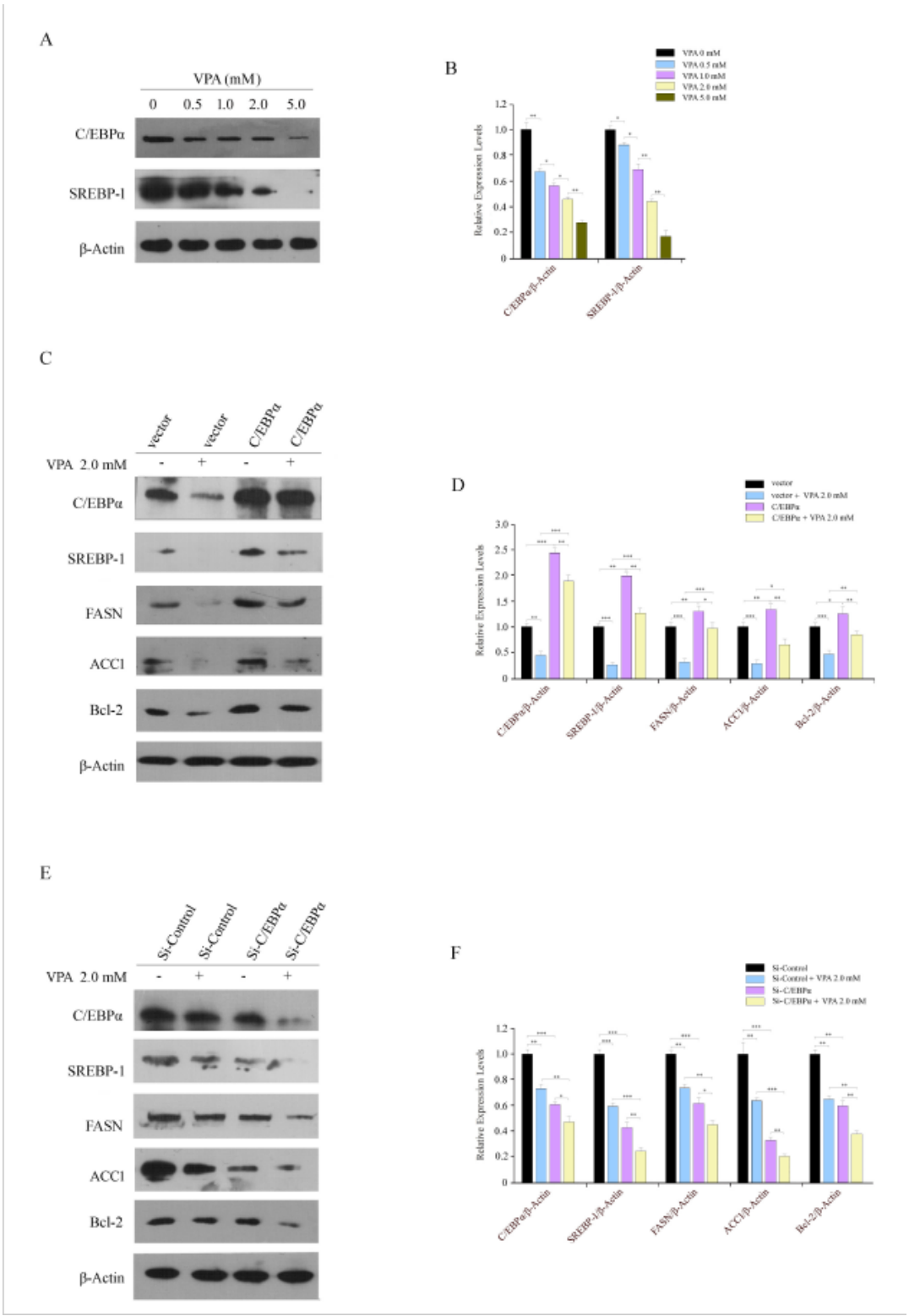

Figure 4

C/EBPα regulated lipogenesis and apoptosis-related genes in VPA-treated PC-3 cells. (a and b) Expression of C/EBPα and SREBP-1 in PC-3 cells treated with various concentrations of VPA was analyzed by Western blotting analysis. The levels of C/EBPα and SREBP-1 were quantified by densitometry and

normalized with those of β-Actin. (c and d) PC-3 cells were transfected with C/EBPα-expressing plasmid, followed by treatment with or without 2.0 mM VPA for 48 h. The levels of C/EBPα, SREBP-1, FASN, ACC1, and Bcl-2 were measured by Western blotting analysis. The fold-change was calculated based on a densitometric analysis of the band intensities. Mock: The cells were transfected with empty plasmid. (e and f) PC-3 cells were transfected with Si-C/EBPα, followed by VPA treatment. The levels of C/EBPα, SREBP-1, FASN, ACC1, and Bcl-2 were measured by Western blotting analysis. Mock: The cells were transfected with scrambled control si-RNA (Si-Control). Statistically significant differences are indicated as fellows: NS (no significance), *P < 0.05, **P < 0.01, and ***P < 0.001.

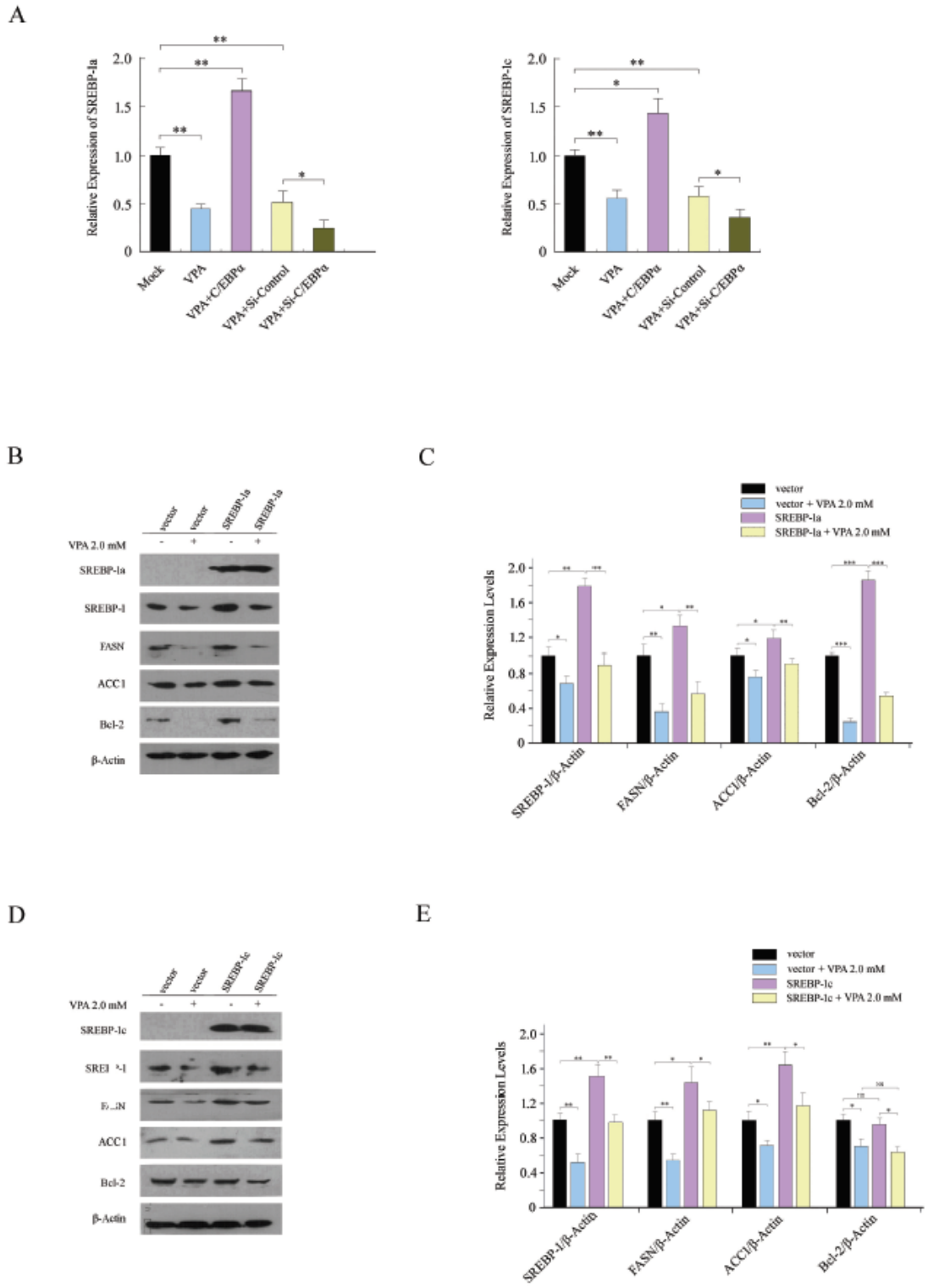

Figure 5

Effects of SREBP-1a and SREBP-1c on expression of lipogenesis and apoptosis-related genes in VPA-treated PC-3 cells. (a) qRT-PCR analysis of the mRNA levels of SREBP-1a and 1c in PC-3 cells after transfection with C/EBPα or Si-C/EBPα and treatment with or without VPA. β-Actin was used for normalization. (b and c) PC-3 cells were transfected with SREBP-1a-expressing plasmid, followed by treatment with or without 2.0 mM VPA. The protein expression in treated cells was determined by Western

blotting analysis. β-Actin was used as an internal reference. (d and e) Expression levels of SREBP-1, FASN, ACC1, and Bcl-2 were analyzed by Western blotting analysis in VPA-treated PC-3 cells after transfection with SREBP-1c.

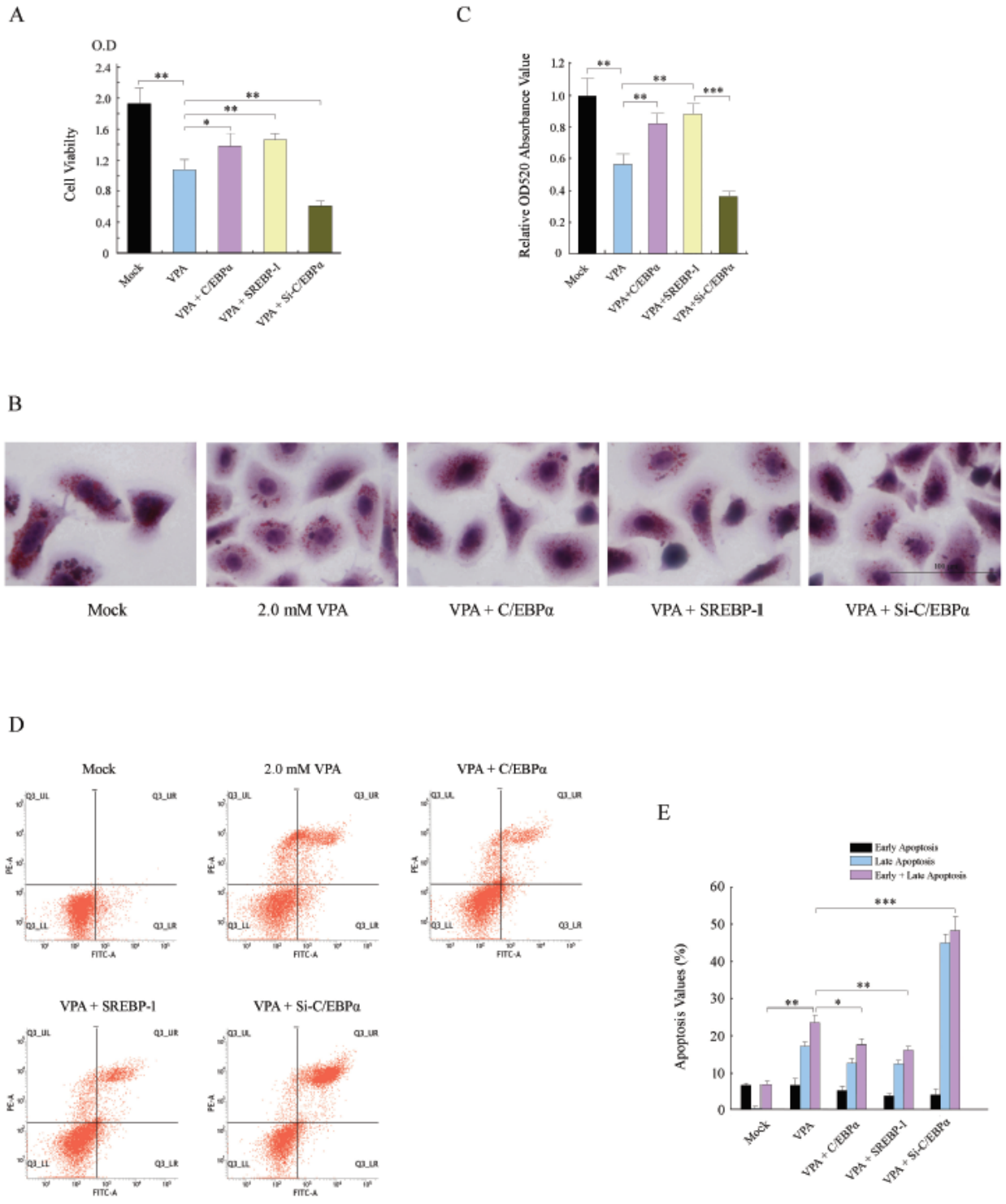

Figure 6

Effects of the C/EBPα/SREBP-1 pathway on lipogenesis and apoptosis in VPA-treated PC-3 cells. (a) PC-3 cells were transfected with an expressing plasmid encoding C/EBPα or SREBP-1a/c, Si-Control, or Si-

C/EBPα, followed by treatment with or without 2.0 mM VPA. The cell viability was determined using MTT cell viability assay. (b) Representative microscopic images of Oil-Red O staining of PC-3 cells transfected with C/EBPα- or SREBP-1-expressing plasmid or Si-C/EBPα following treatment with VPA (2.0 mM) for 48 h. (c) Oil-Red O extracted with isopropanol was measured at OD520. (d) Representative scatter plots of flow cytometric cell viability measurement on PC-3 cells under different treatments. (e) Percentages of apoptotic cells were quantified and graphed. The values represent the mean ± S.D of three experiments. Statistically significant differences are indicated as fellows: NS (no significance), *P < 0.05, **P < 0.01, and ***P < 0.001.